CRASH DETECTION METHOD FOR MOTORCYCLE AIRBAG SYSTEM WITH SENSORS ON THE FRONT FORK

Yuki Kobayashi
Takumi Makabe
Motorcycle R&D Center/Honda R&D Co., Ltd.
Japan
Paper Number 13-0113

ABSTRACT

Honda's previous motorcycle airbag system employs a crash detection method to deploy the airbag according to signals the system receives from four accelerometers where two of them installed on each of the front suspension fork legs. However, the system can be used only on models with larger vehicle sizes due to larger area required for the installation of the four sensors.

This paper describes the development of a method to overcome the space limitations of the prior method. In developed method, the crash detection can be carried out by only two sensors where one of them installed on each front suspension fork leg. This makes it possible to apply an airbag system to other motorcycle models as well.

In this developed method, the threshold value, which is used for crash discrimination, is processed as a function of longitudinal displacement of the front suspension. At each time step in the discrimination execution processes, the deceleration value is compared with the threshold processed as described above.

Through the analysis using spectrogram, it was revealed that the accelerometer outputs, when traveling on rough roads, show sinusoidal oscillation waves derived from the natural oscillation of the system composed of the front wheel and the suspensions. Consequently, waveforms of the longitudinal deceleration and the displacement, where the displacement is calculated by the second order integration of the deceleration, show the opposite phase to each other. On the other hand, in a frontal impact, the output of the accelerometer is generally expressed by the approximation of a half sine wave. Accordingly, the displacement from a frontal impact shows a monotonic increase. Utilizing these characteristics, a two-sensor crash detection method has been developed.

The developed method was evaluated using data measured in various tests, including full-scale impact tests and rough roads tests, using large touring motorcycles and large scooters.

INTRODUCTION

Motorcycle airbag exploratory studies began in the 1970's. Early works addressed the crash detection necessary to trigger airbag deployment as well as the airbag concepts themselves. Sporner et al examined the usefulness of a crash detection system that utilized the sound emitted when front suspension is deformed during an impact [1]. Chinn et al analyzed acceleration data obtained from sensors mounted at different locations on a motorcycle to identify the characteristics of sensor outputs for a trigger system [2]. In these previous studies, preliminary crash detection methods were proposed based on the impact measurements on the system composed of the front wheel and the suspensions (front wheel-suspension system). However, those researches did not include the practical issues associated with the actual system application for a motorcycle.

In the 1960s, Honda began its research, aiming to enhance rider protection, and its research on motorcycle airbag systems has been seen by some as a significant breakthrough.

In an early exploratory study on a large touring motorcycle, a prototype triggering device was used [3]. The device consisted of an electric control unit and an accelerometer located near the front axle on each of the two front suspension fork legs. The signals from the accelerometers were calculated separately to generate the triggering signals and the airbag was triggered by the earlier signal.

As another example, a preliminary study of an impact sensing system for a large scooter was conducted [4]. On each front suspension fork leg, an accelerometer was installed and the other accelerometer was located on the front cowl framework. Two crash detection

processes were applied. One of them used the averaged value of signals from the two accelerometers on the front suspension fork legs, while the other used the signal from the accelerometer on the front cowl frame. The airbag was triggered when either one of the two processes indicate a moderate to severe frontal impact.

Based on these studies of various kinds of detection methods, Honda decided to apply a crash detection method that used the signals from a total of four accelerometers, a pair on each front suspension fork leg. The first production airbag system incorporating this method was introduced on the 2006 Honda Gold Wing. Figure 1 shows the airbag system configuration applied to the Gold Wing.

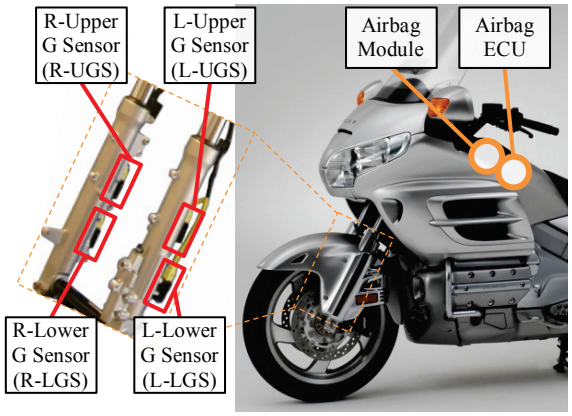

Figure 1. Previous Motorcycle Airbag System Configuration.

The front wheel-suspension system is the part of the motorcycle that experiences the initial impact forces in a typical motorcycle frontal collision. Because of this, the crash deceleration pulse from the right and the left front suspension fork legs are utilized in the crash detection system.

Within existing motorcycle structures, the space for installation of accelerometers depends on the structure of the base model. For example, suspension arrangements (normal telescopic, inverted, trailing link etc.), suspension length, and pre-installed peripheral devices, such as brake calipers, limit the available space to install accelerometers. Therefore, this method only is applicable to a limited number of models which have a space large enough to install two sensors on each front suspension fork leg.

The current study was intended to help overcome these limitations with the result being that it was possible to develop a crash detection method using a total of just two accelerometers, one each on the right and the left front suspension fork legs. This was made possible by extracting the characteristics of deceleration waveforms measured at the front suspensions in a crash and during normal operation.

MOTORCYCLE CRASH DETECTION METHOD

Table 1 shows the major specifications of the large touring motorcycle used for our study.

Table 1.
Specifications of the test motorcycle

Length	(mm)	2,630
Width	(mm)	945
Height	(mm)	1,525
Wheelbase	(mm)	1,690
Curb Mass	(kg)	425
Engine Displacement	(cm^3)	1,832

Crash Detection Method for Previous Motorcycle Airbag System

Figure 2 shows the block diagram of crash detection for the previous motorcycle airbag system.

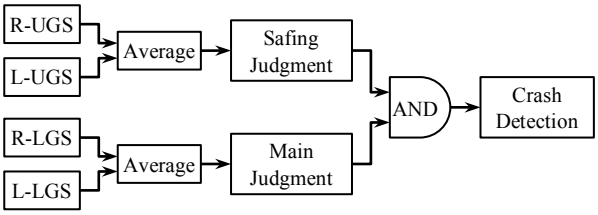

Figure 2. Block Diagram of Previous Crash Detection.

The Main Judgment portion discriminates whether a sufficiently severe crash requiring deployment of the airbag has occurred. The Safing Judgment portion is a failsafe function to prevent undesired deployment of the airbag that might be caused by the failure of, or an erroneous signal from, the accelerometer configuring the Main Judgment.

Right and Left Averaging and the Safing Judgment

The previous crash detection method adopts the Main and Safing Judgments based on the average of the signals from the right and the left accelerometers. The averaging processes can reduce the effect caused by the front wheel-suspension system being forcefully steered by the impact at the early stage of a crash. As an example, Figure 4 shows the deceleration signals measured at the front suspension fork legs in the two ISO13232 [5] impact configurations shown in Figure 3.

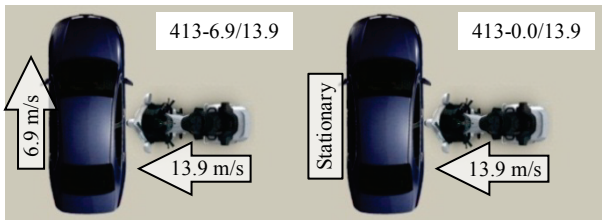

Figure 3. Impact Test Configurations Defined in ISO13232.

The impact configuration code comprises a series of three digits describing the opposing vehicle contact point, the motorcycle contact point, and relative heading angle, respectively, followed by the opposing vehicle impact speed, and the motorcycle impact speed.

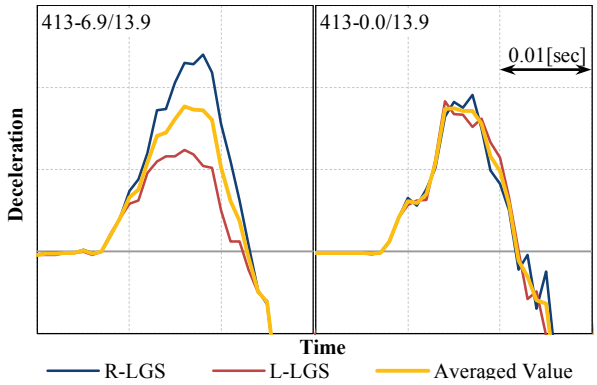

Figure 4. Comparison of R/L-LGS Deceleration.

While R-LGS deceleration value is equivalent to L-LGS deceleration value in the stationary car impact configuration 413-0.0/13.9, the deceleration value of L-LGS is lower than that of R-LGS in the both moving impact configuration 413-6.9/13.9. This is because the front wheel-suspension system was forcefully steered by impact with the opposing vehicle that was moving in a lateral direction relative to the motorcycle. However, the averaged value of the deceleration values from R-LGS and L-LGS is equivalent in both impact configurations. Consequently, by the use of the averaging process, the effect of the steered front wheel is significantly reduced.

The Main Judgment, which is based on the averaged signals from R-LGS and L-LGS, detects a crash erroneously when one of LGSs outputs a high deceleration value due to malfunction of, or an erroneous signal from the accelerometer. The Safing Judgment is provided in order to reduce the probability of an undesired deployment of the airbag due to failure of the accelerometer, or the like, during normal operation. With the previous airbag system, an additional pair of accelerometers (R/L-UGS) is installed on the right and the left front suspension fork legs for the Safing Judgment, which is, again, based on the averaged value of the two figures. As crash detection is made by the logical conjunction of the Main Judgment and the Safing Judgment, even if any one of the Judgments detects a crash by the failure, or the like, of one accelerometer, the other Judgment prevents an improper deployment signal to the airbag.

Two-Sensor Crash Detection

Based on the previous crash detection method, with R/L-UGS removal, we developed a two-sensor crash detection, the block diagram of which is shown in Figure 5.

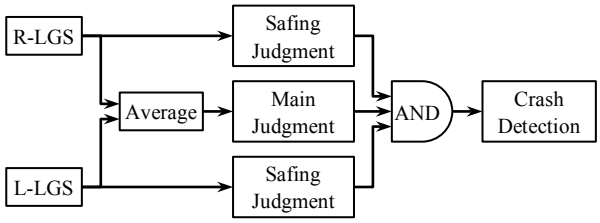

Figure 5. Block Diagram of Two-Sensor Crash Detection.

With this configuration, if an output abnormality occurs in R-LGS, because the Main Judgment is calculated with the averaged value of LGSs outputs, it may incorrectly detect that a crash has occurred. And besides, one of the Safing Judgments, which is calculated with R-LGS output, may also output an improper ON signal. However, because the other Safing Judgment, which is calculated with L-LGS output, is OFF, an undesired deployment can be avoided.

In the two-sensor crash detection system, the Main Judgment has the comparable performance of discrimination because the same judgment process is applicable as in the previous system. On the other hand, the Safing Judgment is based on the individual signals from R-LGS and L-LGS and they are affected by the steered motion of the front wheel as described above. Therefore, the same judgment process cannot be applied as in the previous system. That is why we needed to develop a different method for our system.

The target performance for the Safing Judgments is to output OFF signals at all times in normal operations including rough road running and to output ON signals at the time when a crash requires the airbag to be deployed. The waveforms measured when running along rough roads are shown in Figure 6 as an example of the situations where OFF judgment is required. As

shown in the graph, the spikes of high deceleration can be observed and these are considered as sudden decelerations when the front tire experiences the impacts when the vehicle runs over the edges of potholes.

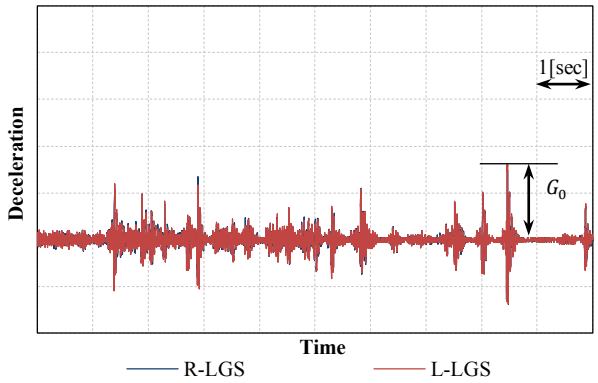

Figure 6. Deceleration Time History in Rough Road Running.

In the next step, a collision where a passenger vehicle impacts a motorcycle while the rider is waiting to turn left is simulated as an example of a situation where ON judgment is required. The waveforms measured in such a collision are shown in Figure 7.

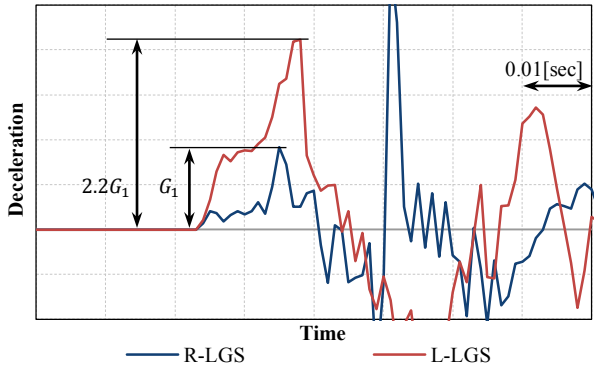

Figure 7. Deceleration Time History in Steered Collision.

The scales of the vertical axes (Deceleration) of Figure 6 and Figure 7 are the same. There is a difference between the measured decelerations of R-LGS and L-LGS, which reaches the maximum of 2.2 times, caused by the collision accompanying the left-steered state.

The deceleration peak of R-LGS (G_1) shown in Figure 7 is at the same level as the deceleration peak (G_0) during rough road running, which is shown in Figure 6. Therefore it was found that the Safing Judgment is difficult by only comparing the peak deceleration values.

Characteristics of Displacement-Deceleration Curve

In the waveform measured during rough road running shown in Figure 6, the waveform in the vicinity of peak value is shown in Figure 8.

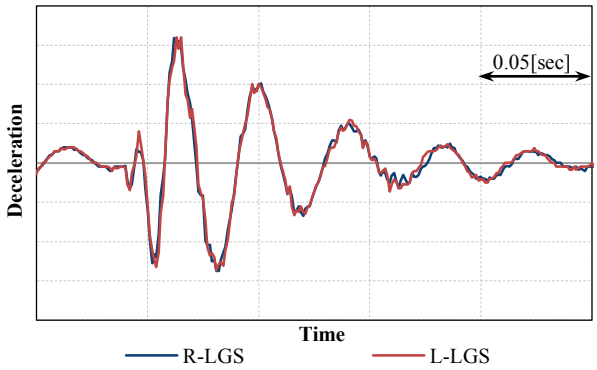

Figure 8. Oscillation Waveform of Front Suspensions.

The spectrogram of measured deceleration value is shown in Figure 9 (a) and (b).

The vertical axis of the figure indicates the frequency, the horizontal axis indicates the time of the measurement, and the colors of the pixels indicate the intensity of the signals.

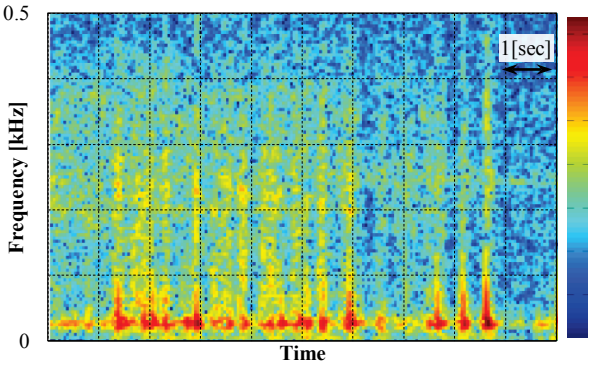

(a) R-LGS

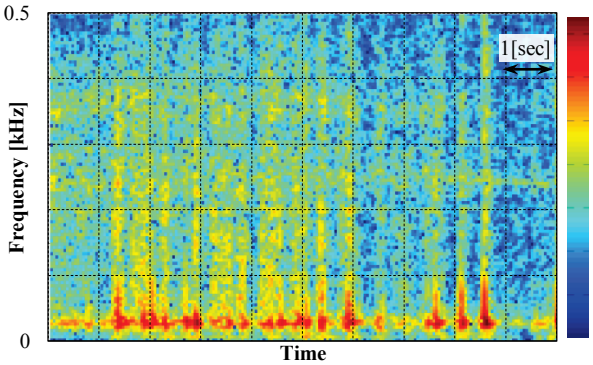

(b) L-LGS

Figure 9. Spectrogram of Rough Road Running Deceleration.

The spectrogram shows high density in a fixed low frequency area around 0.02 kHz even though the random-like exciting forces applied to the front wheel-suspension system with the uneven road surfaces in the rough road running. This low frequency area is almost close to of the natural frequency of the front wheel-suspension system. As the direction of the sensing axis of the accelerometer is orthogonal to the stroke direction of the front suspension, the acceleration along the axis of the suspension, which is caused by the suspension stroke absorbing the road unevenness, is not detected by the accelerometers. On the other hand, the front wheel-suspension system with cantilever structure is excited back and forth by the road unevenness in an orthogonal direction to the stroke of the front suspension. The oscillation period during rough road running is determined by the front wheel-suspension system characteristics regardless of the road unevenness.

We have made the same frequency analysis on the deceleration measured at the occurrence of steered collision (Figure 10).

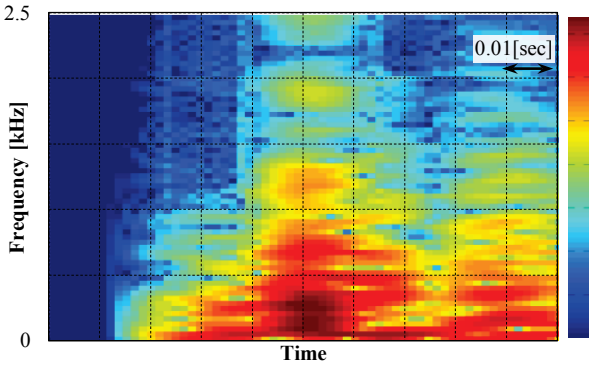

(a) R-LGS

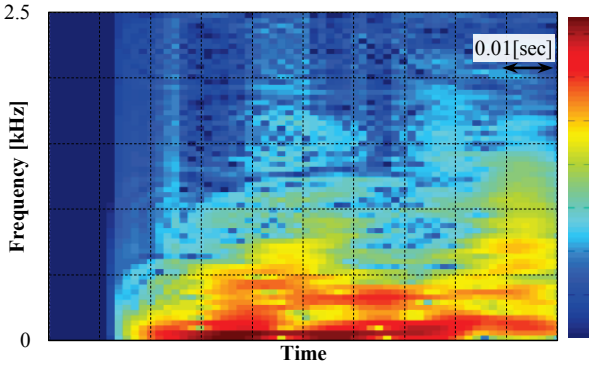

(b) L-LGS

Figure 10. Spectrogram of Steered Collision Deceleration.

As the front fork is deformed over the elastic region during a steered collision, the detected waveform is not dependent on the natural oscillation. As a result, the spectrum dispersed over the wide area below 1.0 kHz.

Based on the result of measured waveform examination, we have verified the Safing Judgment with waveforms that approximate the deceleration measured in the actual tests. The deceleration waveform measured when running rough roads is approximated by the equation (1) as a damped oscillation.

$$m\ddot{x} = -kx - c\dot{x} \quad (1).$$

Where

m : Mass
k : Spring constant
c : Damping coefficient

Assuming initial position as $x(0) = 0$ and initial velocity as $\dot{x}(0) = v_0$, the real root is as follows:

$$x(t) = \frac{v_0}{\sqrt{1-\zeta^2}\omega_0} e^{-\zeta\omega_0 t} \sin\left(\sqrt{1-\zeta^2}\omega_0 t\right) \quad (2).$$

$$\ddot{x}(t) = -\frac{v_0\omega_0}{\sqrt{1-\zeta^2}} e^{-\zeta\omega_0 t} \sin\left(\sqrt{1-\zeta^2}\omega_0 t + 2\varphi\right) \quad (3).$$

Where

$$\zeta = \frac{c}{2\sqrt{mk}}$$

$$\omega_0 = \sqrt{\frac{k}{m}}$$

$$\varphi = \tan^{-1}\left(\frac{\zeta}{\sqrt{1-\zeta^2}}\right)$$

We determined each parameter experimentally from the results of measurements in actual running tests, and obtained the approximate waveform shown in Figure 11.

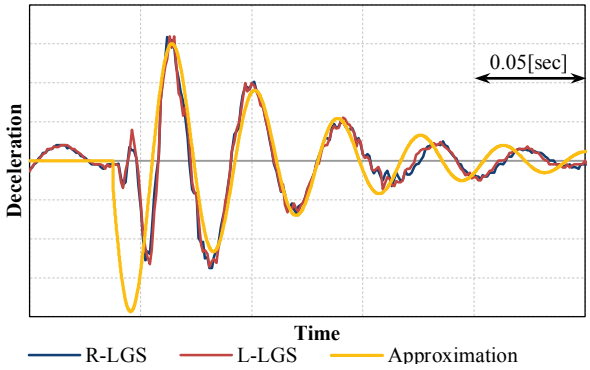

Figure 11. Approximation of Oscillation of Front Suspension.

The damping coefficient was $\zeta = 0.08$. Assuming $\varphi \simeq 0$ from $\zeta \ll 1$, equation (4) can be obtained from equation (2) and equation (3).

$$\ddot{x}(t) \simeq -\omega_0^2 x(t) \tag{4}$$

The acceleration represents an oscillation almost reverse in phase to the displacement.

On the other hand, the initial deceleration pulse in a steered collision is approximated by the equation (5) as a half-sine wave.

$$\ddot{x}(t) = \begin{cases} 0 & (t < 0) \\ a_0 \sin \omega t & (0 \le t \le \pi/\omega) \end{cases} \tag{5}$$

The displacement is expressed by equation (6).

$$x(t) = \begin{cases} 0 & (t < 0) \\ a_0(\omega t - \sin \omega t)/\omega^2 & (0 \le t \le \pi/\omega) \end{cases} \tag{6}$$

The approximate waveform of R-LGS, which is shown in Figure 7, is shown in Figure 12 when the constants of a_0 and ω are assumed the same as in those of the damped oscillation in equation (3).

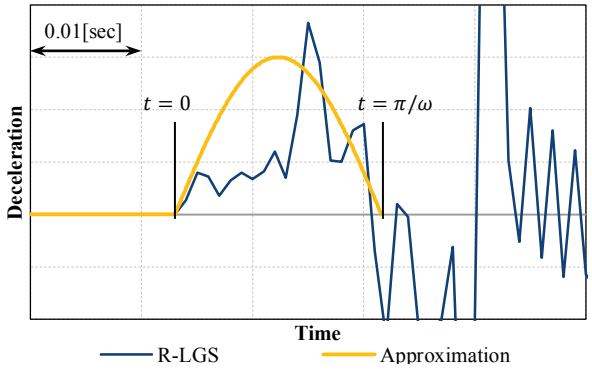

Figure 12. Approximation of Deceleration of Steered Collision.

Regarding these approximate waveforms, the displacement-deceleration curves are shown in Figure 13 with the vertical axis defined as deceleration and horizontal axis defined as displacement.

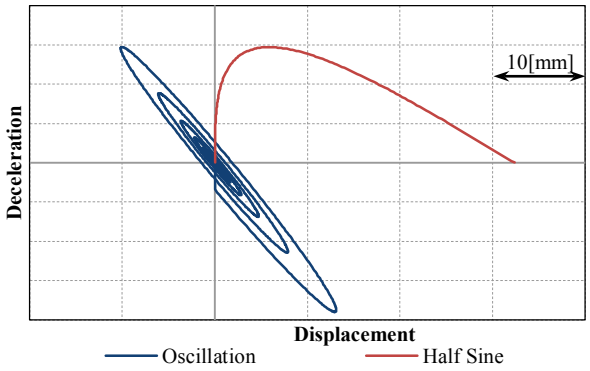

Figure 13. Displacement-Deceleration Curves of Approximations.

Distribution of the damped oscillations is situated over the second and fourth quadrants as the displacement and the deceleration have the opposite phases to each other. On the other hand, distribution of the half-sine wave is situated in the first quadrant as the displacement increases monotonically. By utilizing these characteristic, it becomes possible to distinguish between the rough road running and a steered collision with an appropriate judgment threshold line in the first quadrant of the displacement-deceleration plane.

Application to Crash Detection

Distinction between rough road running and a steered collision by means of displacement-deceleration curves was applied to the Safing Judgment in Figure 5. The displacement-deceleration curves of data, which are measured in rough road running and steered collision, are shown in Figure 14 together with and judgment threshold line.

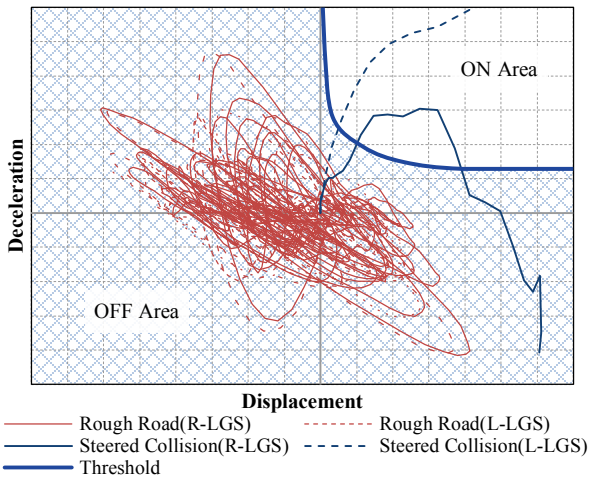

Figure 14. Displacement-Deceleration Curves and Threshold of Two-Sensor Safing Judgment

The first quadrant on the displacement-deceleration plane shows that the status of the front wheel-suspension system is shifted to an area behind the normally located position and is decelerating as well. In this area the ON area was set, because it is translated that the impacts were applied to the extent at which the deformation of the front wheel-suspension system lead to the plastic range and the threshold line shown in Figure 14 was specified. The waveforms when running rough roads and when experiencing the steered collision are distinguishable on the displacement-deceleration plane even though those deceleration peaks reach to the same levels.

VERIFICATION

We compared the ON/OFF judgment results between the previous technology and the two-sensor crash detection method by using the result of the acceleration measured with a large touring motorcycle (Table 2). We have obtained the ON/OFF judgment results equivalent to those obtained using the previous technology in all configurations.

Table 2.
Evaluation result of the two-sensor Safing Judgment

Configurations	Result				
	Main Judgment		Safing Judgment		
	Previous Method	Two Sensor	Previous Method	Two Sensor	
				R	L
Rough Road	OFF	OFF	OFF	OFF	OFF
Low Speed Crash	OFF	OFF	ON	ON	ON
413-0.0/13.9	ON	ON	ON	ON	ON
413-6.9/13.9	ON	ON	ON	ON	ON
Steered Collision	ON	ON	ON	ON	ON

The verification of the method is conducted with a large scooter as well. The vehicle specifications are shown in Table 3.

Table 3.
Specifications of the large scooter

Length	(mm)	2,185
Width	(mm)	750
Height	(mm)	1,180
Wheelbase	(mm)	1,545
Curb Mass	(kg)	204
Engine Displacement	(cm^3)	248

Unlike the large touring motorcycle, the large scooter does not have an upper triple clamp on its front fork and has a smaller front wheel. However, the waveforms measured in the rough road running tests show damped oscillations (Figure 15).

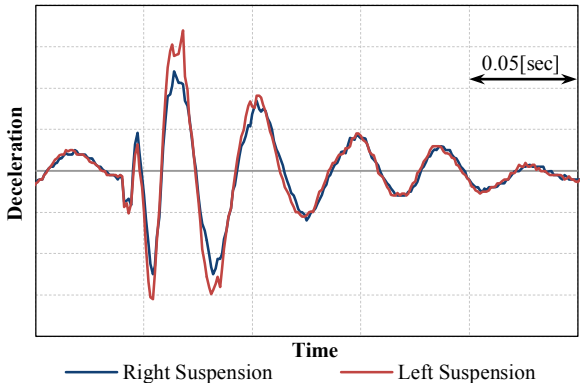

Figure 15. Oscillation Waveform of Front Suspension of Large Scooter in Rough Road Running.

The displacement-deceleration curves of the large scooter, shown in Figure 16, show similar features to those of the large touring motorcycle, even though the parameters of natural oscillation in the large scooter are different from those of the large touring motorcycle because of the difference in the constructions of the front wheel-suspension system.

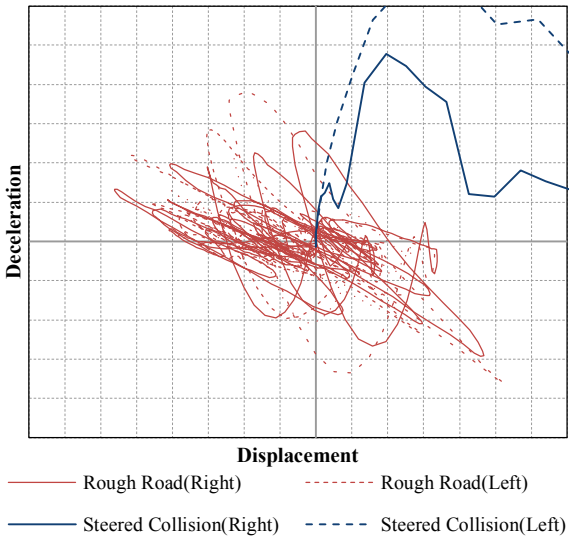

Figure 16. Displacement-Deceleration Curves of the Large Scooter.

CONCLUSIONS

The two-sensor crash detection method was developed to apply to mass-production large motorcycles.

The developed method utilized the characteristics which were investigated through analyses of oscillation

behaviors in motions of front wheel-suspension systems while driving in rough roads and while experiencing impacts in the vehicle collisions.

Following the method development, the validity of the method was confirmed with the equivalent judgment performance obtained in the comparison tests of the previous method with the data measured in the large touring motorcycle.

In addition, it was confirmed that this method was also applicable to the motorcycles with different constructions of the front wheel-suspension system based on the data measured in the large scooters.

REFERENCES

[1] Sporner, A., Langwieder, K., Polauke, J., 1987, "Development of a Safety Concept for Motorcycles - Results From Accident Analysis and Crash Tests." in Proceedings of 11th International Technical Conference on Experimental Safety Vehicles, Washington D.C., 835 - 842.

[2] Chinn, B.P., Okello, J.A., McDonough, P.J., Grose, G., 1996, "Development and Testing of a Purpose Built Motorcycle Airbag Restraint System." in Proceedings of 15th International Technical Conference on the Enhanced Safety of Vehicles, Melbourne, Paper Number 96-S7-O-13.

[3] Iijima, S., Hosono, S., Ota, A., Yamamoto, T., 1998, "Exploratory Study of an Airbag Concept for a Large Touring Motorcycle." in Proceedings of 16th International Technical Conference on the Enhanced Safety of Vehicles, Paper Number 98-S10-O-14.

[4] Kuroe, T., Iijima, S., Namiki, H., 2004, "Exploratory Study of an Airbag for a Large Scooter-Type Motorcycle." in Proceedings of 5th International Motorcycle Conference 2004, Munchen.

[5] International Organization for Standardization, 2005, "Motorcycles - Test and analysis procedures for research evaluation of rider crash protective devices fitted to motorcycles -." International Standard ISO 13232 2005(E)